Development 129, 1215-1223 (2002)
Printed in Great Britain © The Company of Biologists Limited 2002
DEV5980

Drosophila myosin phosphatase and its role in dorsal closure

Tomoaki Mizuno[1,2], Kyoko Tsutsui[1] and Yasuyoshi Nishida[1,*]

[1]Division of Biological Science, Graduate School of Science, Nagoya University, Chikusa-ku, Nagoya 464-8602, Japan
[2]CREST, Japan Science and Technology Corporation, Honmachi, Kawaguchi, Saitama 332-0012, Japan
*Author for correspondence (e-mail: nishida@bio.nagoya-u.ac.jp)

Accepted 12 December 2001

SUMMARY

Myosin phosphatase negatively regulates nonmuscle myosin II through dephosphorylation of the myosin regulatory light chain (MRLC). Its regulatory myosin-binding subunit, MBS, is responsible for regulating the catalytic subunit in response to upstream signals and for determining the substrate specificity. DMBS, the *Drosophila* homolog of MBS, was identified to study the roles of myosin phosphatase in morphogenesis. The embryos defective for both maternal and zygotic *DMBS* demonstrated a failure in dorsal closure. In the mutant embryos, the defects were mainly confined to the leading edge cells which failed to fully elongate. Ectopic accumulation of phosphorylated MRLC was detected in lateral region of the leading edge cells, suggesting that the role of DMBS is to repress the activation of nonmuscle myosin II at the subcellular location for coordinated cell shape change. Aberrant accumulation of F-actin within the leading edge cells may correspond to the morphological aberrations of such cells. Similar defects were seen in embryos overexpressing Rho-kinase, suggesting that myosin phosphatase and Rho-kinase function antagonistically. The genetic interaction of *DMBS* with mutations in the components of the Rho signaling cascade also indicates that DMBS functions antagonistically to the Rho signal transduction pathway. The results indicate an important role for myosin phosphatase in morphogenesis.

Key words: Rho-kinase, MBS, *zipper*, *spaghetti-squash*, Rho, RhoGEF, Morphogenesis, *Drosophila melanogaster*

INTRODUCTION

Morphogenesis is a complex set of processes in which a number of cellular functions such as signal transduction, cell movements, rearrangements and shape changes, are involved. It is desirable to employ model systems for the investigation of such complex processes. Dorsal closure is a morphogenetic event that takes place during the late stages of embryogenesis in *Drosophila melanogaster*. Halfway through embryogenesis, the dorsal surface of the embryo is covered by an extraembryonic membrane, the amnioserosa. Later on, the lateral epidermis stretches dorsally and spreads over the amnioserosa. The two edges of lateral epidermis meet at the dorsal midline and fuse to close the dorsal surface of the embryo. This process is carried out by elongation of the epidermal cells without proliferation or cell recruitment (Martinez-Arias, 1993).

Dorsal closure is a process well suited to studies on the molecular and cellular basis of morphogenesis, and a number of loci involved in this process have been identified from their “dorsal open” or “dorsal hole” phenotypes, which are characterized by large holes in their dorsal cuticle (Noselli, 1998). They can be grouped into at least four classes; genes involved in the Jun amino-terminal kinase (JNK) signaling cascade, genes encoding the components of the Decapentaplegic (Dpp)-mediated signal transduction pathway, genes involved in the Rho GTPase-mediated signaling pathway, and genes encoding cytoskeletal proteins and membrane-associated molecules for cell adhesion. Activation of the JNK signaling cascade is required in the dorsal-most cells of the lateral epidermis, the leading edge cells, to induce the expression of Dpp (Noselli, 1998). One of the target genes of Dpp signaling is *zipper* (*zip*), which encodes the heavy chain of nonmuscle myosin II, and Dpp signaling in the leading edge cells activates the transcription of *zip* (Ariquier et al., 2001).

At the leading edge of the lateral epidermis, filamentous actin (F-actin) and nonmuscle myosin II are prominently accumulated. The supracellular purse-string composed of the actomyosin contractile apparatus provides one of the major forces for promoting dorsal closure (Young et al., 1993). An analysis of the *zip* mutations demonstrated an embryonic lethality due to defects in dorsal closure, indicating that nonmuscle myosin II is required for the morphogenetic processes in dorsal closure (Young et al., 1993). Genetic interactions between *zip* and mutations in the components of the Rho signaling pathway suggest that nonmuscle myosin II is regulated by the Rho signals (Halsell et al., 2000).

Nonmuscle myosin II is a hexamer composed of two of each of three subunits; the heavy chain, the regulatory light chain (MRLC) and the essential light chain. The force-generating activity of actomyosin is mainly regulated by phosphorylation and dephosphorylation of MRLC. Ca^{2+}/calmodulin-dependent myosin light chain kinase (MLCK) and Rho-kinase/Rokα, one of the effectors of the Rho GTPase, are responsible for the

phosphorylation of MRLC (Tan et al., 1992; Amano et al., 1996). However, myosin phosphatase dephosphorylates MRLC, leading to the inactivation of nonmuscle myosin II. Myosin phosphatase is a heterotrimer composed of a catalytic subunit belonging to protein phosphatase 1c (PP1c), the myosin-binding subunit (MBS) and M20 (Alessi et al., 1992; Hartshorne et al., 1998). MBS plays the regulatory roles of myosin phosphatase as a target of the upstream signals and as a determinant of substrate specificity. Myosin phosphatase is negatively regulated through phosphorylation of MBS by Rho-kinase/Rokα (Kimura et al., 1996; Kawano et al., 1999). Thus, Rho-kinase/Rokα doubly activates nonmuscle myosin II through direct phosphorylation of MRLC and inactivation of myosin phosphatase by phosphorylating MBS (Kaibuchi et al., 1999).

We have previously identified the *Drosophila* homolog of Rho-kinase that is encoded by *DRhk*, and have demonstrated that DRho-kinase associates with the GTP-bound DRho1 and phosphorylates the vertebrate MRLC and MBS (Mizuno et al., 1999). Recently, the same gene has been characterized genetically as *Drok*, and has been demonstrated to be involved in the establishment of planar polarity in adult structures such as the compound eye and wing (Winter et al., 2001). We have identified the *Drosophila* homolog of MBS to elucidate the functions of myosin phosphatase in morphogenesis, revealing that MBS functions in dorsal closure and that it acts antagonistically to the Rho signaling cascade and its effector Rho-kinase.

MATERIALS AND METHODS

Fly stocks and culture

l(3)72Dd^{3} (*DMBS^{E1}*), *l(3)72Dd^{03802}* (*DMBS^{P1}*), *Df(3L)th117*, *DRhoGEF2^{04291}*, *zip^{2}*, *zip^{02957}*, *69B-GAL4*, *arm-GAL4* and the blue balancer (*TM3, P[ry$^{+t7.2}$=HZ2.7]DB2*) were obtained from the Bloomington Stock Center, and *EP(3)3727* (*DMBS^{P2}*) was obtained from the Szeged Stock Center. *DMBS^{P2r31}* was derived from *DMBS^{P2}* by imprecise excision of the *P*-insertion. *DRho1^{72BH}* and *DRho1^{72O}* (Strutt et al., 1997), and *zip^{Ebr}* (Gotwals and Fristrom, 1991) were provided by M. Mlodzik and J. Fristrom, respectively. *Drok^{2}* (Winter et al., 2001) and GFP-Sqh (Sisson et al., 2000) were provided by L. Luo and R. Karess, respectively. Fly cultures and crosses were carried out at 25°C unless otherwise stated.

Cloning of *DMBS* cDNA

PCR primers were designed on the basis of the DNA sequences of two EST clones (GH27673 and GM02173) sequenced by the Berkeley *Drosophila* Genome Project. The primer sequences are 5′-AGC-AATAGCGATACAACAGCGCTAC-3′ and 5′-GGTACCGTCTGCT-TATCTTAACGTACTC-3′. Two embryonic cDNA libraries (Brown and Kafatos, 1988) were used as templates. Pyrobest DNA polymerase (Takara Shuzo Co. Ltd., Japan) was used for PCR, which was performed according to the following protocol: 30 cycles of 94°C for 15 seconds, 55°C for 30 seconds, and 70°C for 5 minutes. The PCR products were cloned into pBluescript and sequenced.

Generation of an antibody to DMBS and immunoblotting

A rabbit polyclonal anti-DMBS-C1 antibody was raised against a synthetic polypeptide, KEKESGSERTSRS, corresponding to the carboxyl-terminal portion of DMBS shared by DMBS-L and DMBS-S, and was affinity purified. The polyclonal antibody and the mouse monoclonal anti-Pnut antibody (Neufeld and Rubin, 1994) obtained from the Developmental Studies Hybridoma Bank were used for immunoblotting after dilution to 1/700 and 1/20, respectively. Sqh, the *Drosophila* homolog of MRLC, and its phosphorylated form were detected using the anti-Sqh antibody (Jordan and Karess, 1997) and rabbit polyclonal anti-phospho-MRLC antibody (Matsumura et al., 1998), respectively, as described (Winter et al., 2001). The latter antibody has been raised against a synthetic peptide based on the mouse sequence, and was provided by F. Matsumura. It reacts with the *Drosophila* protein.

Generation of transgenic lines and rescue of *DMBS* mutants

The *DMBS-L* and *-S* cDNAs were cloned into pP[CaSpeR-hs] and *hs-DMBS-L* and *hs-DMBS-S* transgenic lines were generated by the standard procedure. For rescue experiments, each two of the independent transgenes of *hs-DMBS-L* or *hs-DMBS-S* on the third chromosome were used, and the transgenes were combined with either *DMBS^{E1}* or *DMBS^{P1}* by recombination. Matings were performed between *w*; *DMBS*/*TM3*, *Sb* and *w*; *DMBS hs-DMBS-L*/*TM3*, *Sb* or *w*; *DMBS hs-DMBS-S*/*TM3*, *Sb*, and the cultures were either kept at 25°C or treated at 37°C for 1 hour twice a day throughout development. The full-length *DRhk^{+}* cDNA was cloned into pUAST (Brand and Perrimon, 1993) to generate *UAS-DRhk^{+}* transgenic lines.

Immunohistochemistry and confocal microscopy

Phalloidin staining

Embryos were fixed for 20 minutes in 7.2% formaldehyde/PBS: heptane, 1:1, and were devitellinized by hand. Embryos were incubated in rhodamine-conjugated phalloidin (Molecular Probes, Inc.) for 20 minutes, and were then washed with 0.2% Triton X-100/PBS three times. The *DMBS* mutant embryos were distinguished from the paternally rescued embryos by using the blue balancer, *TM3, P[ry$^{+t7.2}$=HZ2.7]DB2*.

Immunostaining

Fixation and staining were carried out by the standard procedures. The primary antibodies and dilutions used are as follows. A mouse monoclonal anti-phosphotyrosine antibody (UBI) at a dilution of 1/1000; the rabbit polyclonal anti-myosin heavy chain antibody (Jordan and Karess, 1997), a gift from R. Karess, at a dilution of 1/1000; and the anti-phospho-MRLC antibody (Matsumura et al., 1998) at a dilution of 1/20. The secondary antibodies used were a rhodamine-conjugated anti-mouse IgG antibody (TAGO) or a FITC-conjugated anti-rabbit IgG antibody (Jackson ImmunoResearch Laboratories). The *DMBS* mutant embryos were distinguished as described above.

For the observation of MRLC distribution, the GFP-Sqh transgenic line (Sisson et al., 2000) provided by R. Karess was used. Embryos were fixed for 20 minutes in 4% paraformaldehyde/PBS: heptane, 1:1, and were devitellinized by vigorous shaking for 10 seconds after substitution of the aqueous layer with methanol. Then, embryos were rehydrated twice with 0.2% saponin/PBS for 10 minutes before mounting.

All images were collected on a Zeiss 512 laser scanning confocal microscope and processed with Adobe Photoshop software.

Expression and purification of DMBS recombinant proteins

For the production of GST-fused DMBS-L, the coding sequence of *DMBS-L* was amplified by PCR using the primer set, 5′-TC-TGAATTCATGTCCTCGCTGGACGCACGCAAC-3′ and 5′-GGT-ACCTCATTTACTTAATTTGCTAATTAC-3′, to create the *Eco*RI restriction sites immediately before the first codon. The amplified DNA fragment was cloned into pGEX-3T-1 (Pharmacia) to fuse with GST at the N terminus. The construct was verified by DNA sequencing. Mutagenesis at the putative phosphorylation site in DMBS was done by PCR using the following primers: 5′-AG-GGAGACTCGACGGTCTGCCCAAGGTGTC-3′ and 5′-CCAGGG-

TGACACCTTGGGCAGACCGTCGAG-3′. Purification of the GST-fusion proteins was carried out essentially as described previously (Frangioni and Neel, 1993).

Immunoprecipitation, immunoblotting and in vitro kinase assay

Immunoprecipitation and immunoblotting of the HA-tagged DRho-kinase were performed as described previously (Mizuno et al., 1999). The immunoprecipitated DRho-kinase was incubated with 0.6 μg of GST-fused DMBS in the kinase buffer and was assayed as described previously (Mizuno et al., 1999).

RESULTS

Identification of the *Drosophila* homolog of MBS

To identify the *Drosophila* homolog of MBS, we searched the *Drosophila* Genome Database for sequences similar to vertebrate MBSs. The vertebrate MBSs share three conserved domains or motifs: amino-terminal ankyrin-repeats, a centrally located major phosphorylation site, and a carboxy-terminal leucine-zipper motif (Fig. 1A). A BLAST search for the putative open reading frame encoding a sequence similar to the phosphorylation site revealed a genomic fragment flanked by sequences encoding ankyrin repeats and a leucine zipper motif.

Analysis of the corresponding EST clones generated by the Berkeley *Drosophila* Genome Project revealed that none of them contained all three conserved domains. So, we predicted the 5′- and 3′-UTR sequences from the EST and genomic sequences, and amplified the cDNA fragments containing the complete coding sequence by PCR using cDNA libraries for templates (see Materials and Methods). Two types of cDNAs were thus obtained from different cDNA libraries, each encoding a polypeptide of 927 and 797 amino acid residues with the predicted relative molecular mass of 101,409 and 87,509, respectively. The two sequences are identical except for an insertion of a 129 amino acid sequence upstream of the putative phosphorylation site in the longer polypeptide (Fig. 1A).

They contained the three conserved motifs, and the amino acid identities to their corresponding regions of human MYPT2 (Fujioka et al., 1998) are 57.8%, 55.6% and 77.8%, respectively, from the amino terminus (Fig. 1A). The similarity to vertebrate MBSs is restricted to these regions. Vertebrate MBSs and the homolog of *Caenorhabditis elegans*, MEL-11, contain seven ankyrin repeats (Fujioka et al., 1998; Wissmann et al., 1997), but the sequences in the fourth and seventh repeats diverged in *Drosophila*. In the *Drosophila* Genome Database, no other sequence similar to MBS was found, and we consider them as *Drosophila* homologs of MBS. We refer to the longer and shorter forms as *Drosophila* MBS-long (DMBS-L) and *Drosophila* MBS-short (DMBS-S), respectively (Fig. 1A).

The two cDNAs should derive from a single gene by alternative splicing (Fig. 3A). The DMBS-L-specific, 7th exon encodes a sequence of 129 amino acid residues. Furthermore, two in-frame consecutive splicing acceptor sites are present 5′ of the 4th exon (data not shown), and splicing variations at this site added one more amino acid residue in DMBS-L as compared to DMBS-S. We also obtained several partial cDNA fragments different from DMBS-L and DMBS-S (data not shown). Thus, the *DMBS* gene encodes multiple forms of DMBS through differential splicing. Splicing variants have been reported also for the vertebrate MBSs and MEL-11 of *C. elegans* (Hartshorne et al., 1998; Wissmann et al., 1999).

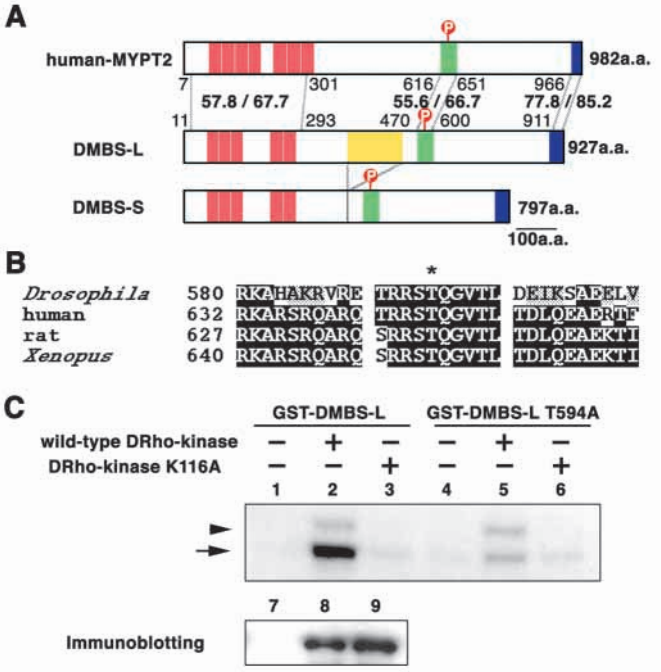

Fig. 1. (A) Schematic representations of basic structural features of DMBS-L (long) and DMBS-S (short) proteins and a comparison with human MBS. The N-terminal ankyrin repeats are indicated in red, and the C-terminal leucine-zipper motif in blue. The sequence specifically found in DMBS-L is shown in yellow. The position of the threonine residue phosphorylated by DRho-kinase is indicated above the rectangles (P), and the conserved region around the phosphorylation site is indicated in green. Human MBS (MYPT2 type a) (Fujioka et al., 1998) is schematically represented above DMBS-L, and the percentages of identity/similarity of the amino acid sequences in the three conserved regions are indicated between the two upper rectangles. The GenBank accession numbers for *DMBS-L* and *–S* cDNAs are AY048675 and AY048676, respectively. (B) A comparison of the amino acid sequence around the putative phosphorylation site of DMBS with those of the vertebrate MBSs. The amino acid residues with positional identity are in white type on black, and the residues with similarity to the vertebrate sequences are shaded gray. The asterisk indicates the threonine residue, which has been demonstrated to be phosphorylated by Rho-kinase in vertebrates. (C) Phosphorylation of DMBS by DRho-kinase and identification of its phosphorylation sites. The HA-tagged DRho-kinase expressed in 293 cells was immunoprecipitated, and the precipitate was used for in vitro kinase assay with GST-fused DMBS-L proteins as substrates. Lanes 1 to 3; GST-DMBS-L, lanes 4 to 6; GST-DMBS-L T594A, in which Ala was substituted for Thr594. The wild-type DRho-kinase (lanes 2 and 8), kinase-dead DRho-kinase^{K116A} (lanes 3 and 6), and vector alone (lanes 1 and 4) were used for the reactions. The arrow indicates the position of DMBS-L and the arrowhead the position of the autophosphorylated DRho-kinase. Portions of the immunoprecipitates were also tested for amounts of kinase by immunoblotting with an anti-HA antibody (lower panel). Lane 7, vector only; lane 8, wild-type DRho-kinase; and lane 9, DRho-kinase^{K116A}.

Phosphorylation of DMBS by DRho-kinase

Previous studies revealed that DRho-kinase physically interacts with DRho1 in the GTP form and phosphorylates the

vertebrate MBS in vitro (Mizuno et al., 1999; Winter et al., 2001). The sequence at the putative phosphorylation site of MBS is well conserved in DMBS (Fig. 1B), and we tested whether DRho-kinase phosphorylates DMBS in vitro. The GST-fused DMBS-L was expressed and purified from *Escherichia coli*, and was found to be phosphorylated by wild-type DRho-kinase but not by kinase-dead DRho-kinase^{K116A} (Fig. 1C, lanes 2 and 3).

Thr594 may correspond to the major phosphorylation site in vertebrate MBS (Fig. 1B). The threonine residue was replaced with an alanine, and this recombinant DMBS was used as a substrate. As shown in Fig. 1C, the level of phosphorylation was significantly reduced, indicating that Thr594 is the major site phosphorylated by DRho-kinase. It has been reported that mammalian MBS is phosphorylated at several sites by Rho-kinase (Kawano et al., 1999), and there presumably are other phosphorylation sites in DMBS as well.

Expression of *DMBS* during development

The pattern of the expression of *DMBS* during development was analyzed by in situ hybridization using *DMBS-L* as a probe (Fig. 2). A significant amount of *DMBS* mRNA was uniformly detected in blastoderm stage embryos (Fig. 2A), and it would be mostly of maternal origin. *DMBS* is expressed ubiquitously throughout embryogenesis (Fig. 2B,C). In the imaginal discs from third instar larvae, the *DMBS* transcript was uniformly detected (data not shown). Tissue- and stage-specificity of the expression for each isoform remain to be analyzed.

Identification of *DMBS* mutants

From the *Drosophila* Genome Database, *DMBS* was located at the 72D region on the left arm of the third chromosome. The intron/exon structure of *DMBS* was deduced from a comparison between the genomic and cDNA sequences (Fig. 3A). In this region, two P-element insertions, *l(3)72Dd*^{03802} and *EP(3)3727*, have been registered in FlyBase (Fig. 3A). They and an EMS-induced mutation, *l(3)72Dd*^{3}, failed to complement to each other. *l(3)72Dd*^{03802} and *l(3)72Dd*^{3} are lethal during early larval stages, while *EP(3)3727* results in development to adults with a mild wing defect (data not shown). Excision of the *P* insertions reversed the lethal and wing phenotypes of *l(3)72Dd*^{03802} and *EP(3)3727*, respectively, indicating that the *P* insertions caused the mutations. Imprecise excision of the *P* insertion from *EP(3)3727* produced a new mutation, *P2r31*, whose lethal phase spans from the third instar larval to early pupal stages.

A polyclonal antibody against a synthetic polypeptide corresponding to the carboxy-terminal region of DMBS was developed, producing a major band of about 95 kDa and several minor bands on the immunoblot (Fig. 3B). Correspondence of these bands to DMBS-L and -S is not certain at this moment. The amounts of the DMBS proteins were analyzed in the mutants. Mutants heterozygous between *P2r31* and the strong alleles or *Df(3L)th117*, which deletes the region including *DMBS*, survived to third instar larvae, and the amount of DMBS was greatly reduced in the extracts prepared from these larvae (Fig. 3B). The result indicates that the mutations are correlated to the amount of DMBS. MRLC is encoded by *spaghetti-squash* (*sqh*) (Karess et al., 1991), and the levels of its phosphorylated form in the mutants were also examined. As shown in Fig. 3C, the levels of phospho-MRLC are significantly elevated in the mutants, indicating that the activity of myosin phosphatase is decreased in the mutants.

To further confirm that the mutations are at the *DMBS* locus, a rescue experiment was performed. *DMBS-L* and *DMBS-S* cDNAs were driven under the heat shock promoter, and induction of either of them by heat shock significantly complemented the lethality of both *l(3)72Dd*^{03802} and *l(3)72Dd*^{3} (Table 1). This may suggest that, despite the expression of multiple isoforms of DMBS, they are functionally redundant. It is also possible that this functional redundancy is partial, and that overexpression of only one isoform would be sufficient for the viability of the fly.

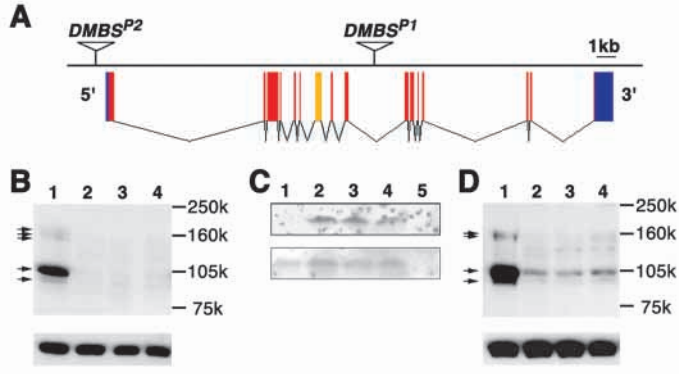

Fig. 3. Identification of the *DMBS* mutations. (A) The genomic structure at the *DMBS* locus. The exon/intron structure is shown with columns and lines under the genomic map. The coding and untranslated regions are indicated as red and blue columns, respectively. The *DMBS-L*-specific exon is represented by a yellow column. The sites of the *P*-element insertions are indicated above the map. (B) Reduction in the amounts of the DMBS proteins in *DMBS* mutants. Protein blots were probed with either an anti-DMBS-C1 antibody (upper panel) or an anti-Pnut antibody (lower panel). Extracts were prepared from late third instar larvae of the following genotypes; wild type (lane 1), *Df(3L)th117*/*DMBS*^{P2r31} (lane 2), *DMBS*^{E1}/*DMBS*^{P2r31} (lane 3), and *DMBS*^{P1}/*DMBS*^{P2r31} (lane 4). Arrows indicate the positions of DMBS bands. (C) Increase of phospho-MRLC in DMBS mutant larvae. The extracts were prepared as described (Winter et al., 2001) from the larvae as in B, except for lane 5 for which *sqh*^{AX3}; *GFP-Sqh* larvae were used. Protein blots were probed with an anti-phospho-MRLC antibody (upper panel) or an anti-Sqh antibody (lower panel). The band corresponding to the GFP-Sqh fusion protein is not included. (D) Reduction in the amounts of DMBS proteins in the *DMBS* mutant females. Protein blots were probed with either an anti-DMBS-C1 antibody (upper panel) or an anti-Pnut antibody (lower panel). The extracts were made from adult females of the following genotypes; wild type (lane 1), *Df(3L)th117*/*DMBS*^{P2} (lane 2), *DMBS*^{E1}/*DMBS*^{P2} (lane 3), and *DMBS*^{P1}/*DMBS*^{P2} (lane 4). Arrows indicate the positions of the DMBS bands.

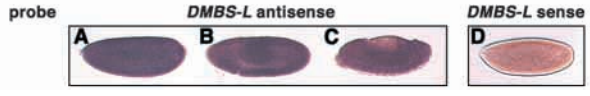

Fig. 2. Expression of *DMBS* during development. Antisense (A-C) or sense RNA (D) probes were used to detect the transcripts. (A,D) Blastoderm embryos, (B) germband-elongated embryo, and (C) germband-retracted embryo. Anterior is to the left and dorsal to the top.

Table 1. Rescue of *DMBS* mutations by transgenic *DMBS-L* or *DMBS-S*

Genotype	– Heat shock	+ Heat shock
$DMBS^{E1}/DMBS^{E1}$	0/167 (0)*	0/110 (0)*
$DMBS^{E1}/DMBS^{E1}$ *hs-DMBS-L*	0/404 (0)	1368/164 (83)
$DMBS^{E1}/DMBS^{E1}$ *hs-DMBS-S*	0/377 (0)	117/195 (60)
$DMBS^{P1}/DMBS^{P1}$	0/262 (0)	0/138 (0)
$DMBS^{P1}/DMBS^{P1}$ *hs-DMBS-L*	0/491 (0)	210/313 (67)
$DMBS^{P1}/DMBS^{P1}$ *hs-DMBS-S*	0/466 (0)	176/245 (72)

*The numerator and denominator represent the number of animals surviving to adulthood and the theoretically expected number of flies with indicated genotype, respectively. The numbers in parentheses represent the respective percentages of surviving flies.

From these results, we conclude that they are the mutations in *DMBS*, and we refer to $l(3)72Dd^{03802}$, *EP(3)3727*, $l(3)72Dd^{3}$ and *P2r31* as $DMBS^{P1}$, $DMBS^{P2}$, $DMBS^{E1}$ and $DMBS^{P2r31}$, respectively. The strength of their phenotype can be ordered as $DMBS^{E1}=DMBS^{P1} > DMBS^{P2r31} > DMBS^{P2}$. Since $DMBS^{E1}$ and $DMBS^{P1}$ gave identical results, only the results obtained with $DMBS^{E1}$ are presented in the following sections unless otherwise mentioned.

Defects in dorsal closure in embryos lacking *DMBS*

The animals homozygous for or transheterozygous between the strong *DMBS* alleles are larval lethal and embryonic development seems to proceed normally (Fig. 7A). This would be because of the maternal contribution of $DMBS^{+}$ activity, a notion consistent with the observation that a significant amount of maternal mRNA is present in early-stage embryos (Fig. 2A). To analyze the function of *DMBS* during embryogenesis, we tried to reduce the maternal contribution.

The mutants transheterozygous between the weak allele, $DMBS^{P2}$, and the strong alleles or *Df(3L)th117*, survived to adults. Examination of such female flies by immunoblotting revealed that the amount of DMBS proteins is greatly reduced (Fig. 3D). When the females transheterozygous between $DMBS^{P2}$ and *Df(3L)th117* were mated with wild-type males, embryonic development proceeded normally in most of the embryos. However, about 25% of the embryos failed to hatch in matings involving males heterozygous for the strong alleles (Fig. 7A). Similar results were obtained with the females of the genotypes, $DMBS^{E1}/DMBS^{P2}$ or $DMBS^{P1}/DMBS^{P2}$ (data not shown). Furthermore, embryonic defects were suppressed by paternal expression of the *DMBS* transgenes (data not shown). These results indicate that embryos fail to develop when *DMBS* is defective both maternally and zygotically, and that the maternal defect is rescued by the paternal expression of a wild-type gene.

About 80% of the dead embryos in the above experiments demonstrated the “dorsal open” or “dorsal hole” phenotype, which can be typically seen in embryos defective in the dorsal closure (Fig. 4B). In the remaining lethal embryos, the pattern of dorsal hairs was disturbed along the dorsal midline (Fig. 4E). These phenotypic variations would be due to the residual activity of maternal *DMBS* derived from the weak allele, $DMBS^{P2}$. The results indicate that DMBS is required in the process of dorsal closure.

Activation and inactivation of nonmuscle myosin II during dorsal closure

To elucidate the roles of DMBS during dorsal closure, the distribution of nonmuscle myosin II and its activation were analyzed during the course of dorsal closure. The process can be divided into three phases. It starts with elongation of the dorsal-most, leading edge cells of the lateral epidermis along the dorsoventral axis. This is followed by elongation of the other lateral epidermal cells with the amnioserosa becoming covered by the elongating epidermis. Finally, the two lateral edges of the epidermis meet at the dorsal midline and fuse to close the epidermis.

Before the onset of the lateral epidermis elongation, the heavy chain of nonmuscle myosin II and MRLC outline the inner surface of the plasma membrane of the lateral epidermal cells at low levels, and they are concentrated at moderate levels along the leading edge of the lateral epidermis (Fig. 5A,B). The phosphorylated form of MRLC is localized similarly (Fig. 5C). During the course of extensive elongation, the heavy chain and MRLC accumulate at high levels along the leading edge (Fig. 5,D,E). Phosphorylated MRLC is also detected at a high level along the leading edge (Fig. 5F). After the meeting of the two lateral epidermal sheets, both the heavy chain and MRLC at the leading edge become diffuse (Fig. 5G,H), and the phosphorylated form of MRLC disappears at the site of fusion (Fig. 5I). These observations indicate that the distribution and phosphorylation of nonmuscle myosin II are dynamically regulated during dorsal closure.

We next examined the distribution and activation of nonmuscle myosin II and F-actin in *DMBS* mutant embryos. Examination of the cell shape with anti-phosphotyrosine antibody revealed that the leading edge cells fail to fully elongate, and some of them remain polygonal (Fig. 6B). In contrast, the epidermal cells located more ventrally elongate nearly normally. A significant amount of phosphorylated MRLC is detected along the dorsal side of the boundaries

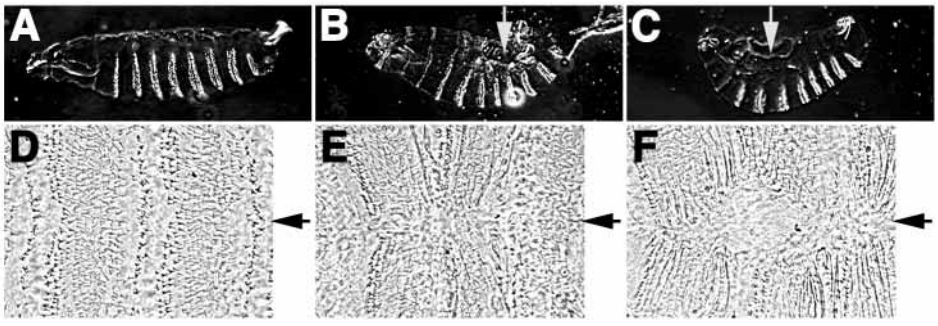

Fig. 4. Defects in dorsal closure in embryos both maternally and zygotically affected in *DMBS* mutants and in embryos overexpressing $DRhk^{+}$. (A,D) Wild type embryos, (B,E) *DMBS* mutant embryos, and (C,F) embryos overexpressing $DRhk^{+}$. (A-C) Embryos viewed with dark-field optics. Anterior is to the left and dorsal up. The arrow indicates the dorsal hole. (D-F) Dorsal views of the lethal embryos without dorsal holes. Arrows indicate the dorsal midline. Anterior is to the left.

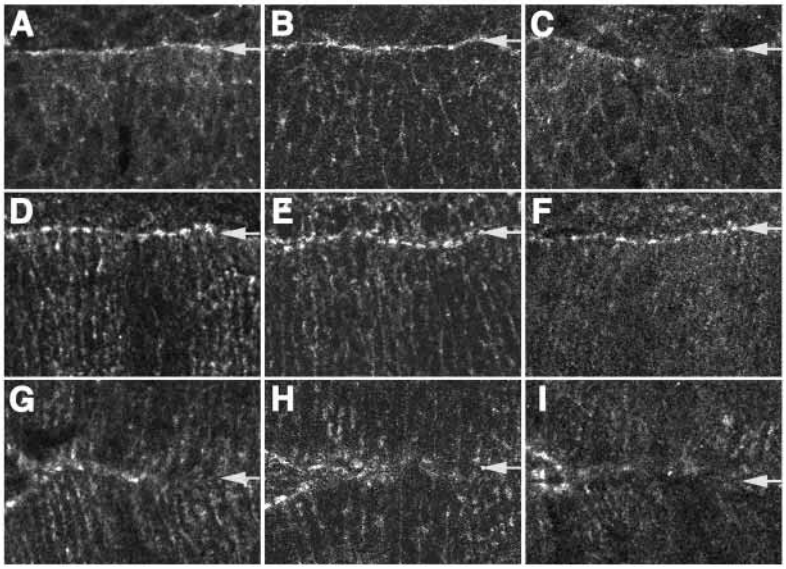

Fig. 5. Distribution of nonmuscle myosin II during dorsal closure. (A-C) Lateral views of embryos before elongation of the lateral epidermis, (D-F) Lateral views of embryos during elongation of the lateral epidermis, and (G-I) Dorsal views of embryos during fusion of the lateral epidermis. Embryos were stained with an anti-myosin heavy chain antibody (A,D,G) or an anti-phospho-MRLC antibody (C,F,I). MRLC was visualized by expression of the GFP-Sqh transgene (B,E,H). Arrows indicate the leading edge of the lateral epidermis in A-F, and the dorsal midline in G-I.

between the leading edge cells in the mutant embryos (Fig. 6J, arrowheads), while the distribution of the heavy chain of nonmuscle myosin II is essentially not affected (Fig. 6H). F-actin is highly accumulated along the leading edge of the lateral epidermis (Fig. 6D). In the mutant embryos, an aberrant accumulation of F-actin within the leading edge cells is observed, while its distribution along the leading edge is essentially unaffected (Fig. 6E). This may correspond to the morphological aberrations of the leading edge cells.

Genetic interactions of *DMBS* with mutations for the heavy chain of nonmuscle myosin and the Rho signaling pathway

DRho-kinase is thought to be responsible for the inactivation of myosin phosphatase through phosphorylation of DMBS. If this inactivation turns out to have a considerable effect on the levels of phosphorylated MRLC, it can be expected that the phenotypes in the *DMBS* mutant embryos and in the embryos overexpressing DRho-kinase would be similar. When *DRhk*$^{+}$ was expressed with the *arm-GAL4* driver, about 80% of the embryos failed to hatch (Fig. 7B). A similar result was obtained with the *69B-GAL4* driver that induces the target gene in the ectoderm (Staehling-Hampton et al., 1994) (data not shown). Most of the lethal embryos showed a dorsal open or dorsal hole phenotype (Fig. 4C), and the pattern of dorsal hairs was disturbed along the dorsal midline in the remaining embryos (Fig. 4F) as observed in the *DMBS* mutant embryos. Examination of the cell shape (Fig. 6C) and the F-actin distribution (Fig. 6F) revealed the same aberrations as those in the *DMBS* mutant embryos.

To examine whether defects in the dorsal closure in the embryos lacking *DMBS* or overexpressing *DRhk*$^{+}$ are due to an aberrant activation of nonmuscle myosin II, the genetic interactions with *zipper* (*zip*), which encodes the heavy chain of nonmuscle myosin II, were analyzed. As already described, about 25% of the progeny from crossing the females transheterozygous with *DMBS*^{P2} and *Df(3L)th117* to the males heterozygous for *DMBS*^{E1} are embryonically lethal (Fig. 7A). We expected that a reduction in the gene dosage of *zip*$^{+}$ would suppress the defects in the *DMBS* mutant or *DRhk*$^{+}$-expressing embryos. When *DMBS*^{P2}/*Df(3L)th117* females are mated with males heterozygous for both *DMBS*^{E1} and *zip*^{Ebr}, half of the embryos defective for both maternal and zygotic *DMBS* should

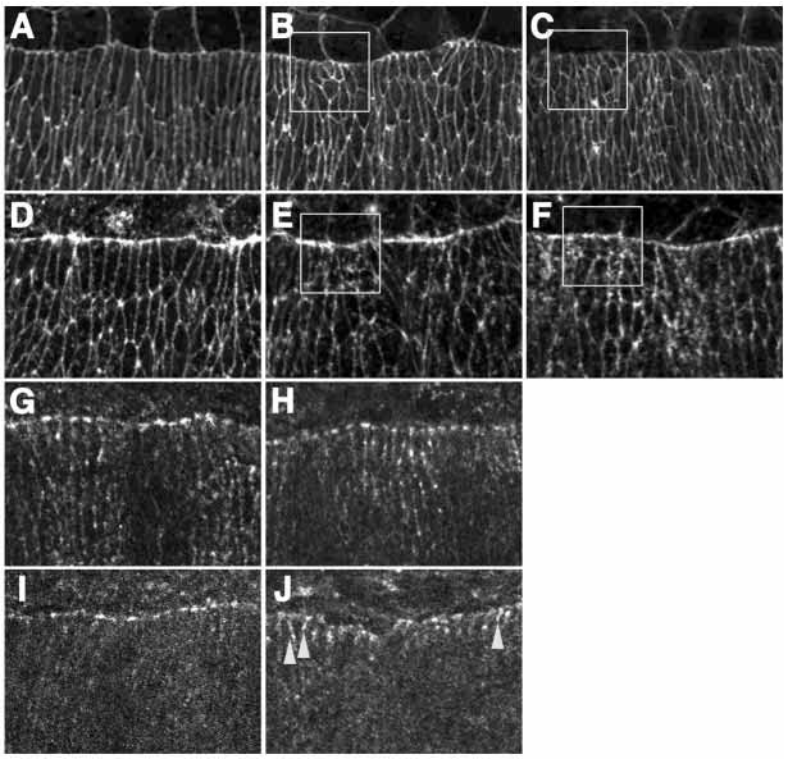

Fig. 6. Cellular aberrations of dorsal closure in *DMBS* mutant embryos and in embryos overexpressing *DRhk*$^{+}$. The wild-type embryos (A,D,G,I), *DMBS* mutant embryos (B,E,H,J) and embryos overexpressing *DRhk*$^{+}$ (C,F) were stained with an anti-phospho-tyrosine antibody (A-C), phalloidin (D-F), an anti-myosin heavy-chain antibody (G,H), and an anti-phospho-MRLC antibody (I,J). The *DMBS* mutant embryos were obtained from a mating between *DMBS*^{P2}/*Df(3L)th117* females and *DMBS*^{E1}/*TM3, P[ry*$^{+t7.2}$*=HZ2.7]DB2* males, and the mutant embryos were identified by use of the blue balancer. *DRhk*$^{+}$ was driven by *69B-GAL4*. The aberrantly distributed phospho-MRLC is indicated with arrowheads in J. Polygonally shaped leading edge cells (B,C) and the leading edge cells with aberrant accumulation of F-actin (E,F) are boxed.

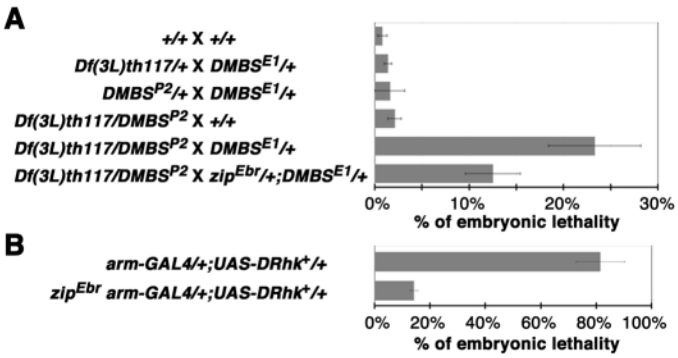

Fig. 7. Lethality in the *DMBS* mutant embryos (A) and in the embryos overexpressing *DRhk*$^{+}$ (B), and the suppression of lethality by *zip*^{Ebr}. Embryonic lethality in the crosses indicated on the left. The maternal (left) and paternal (right) genotypes are given.

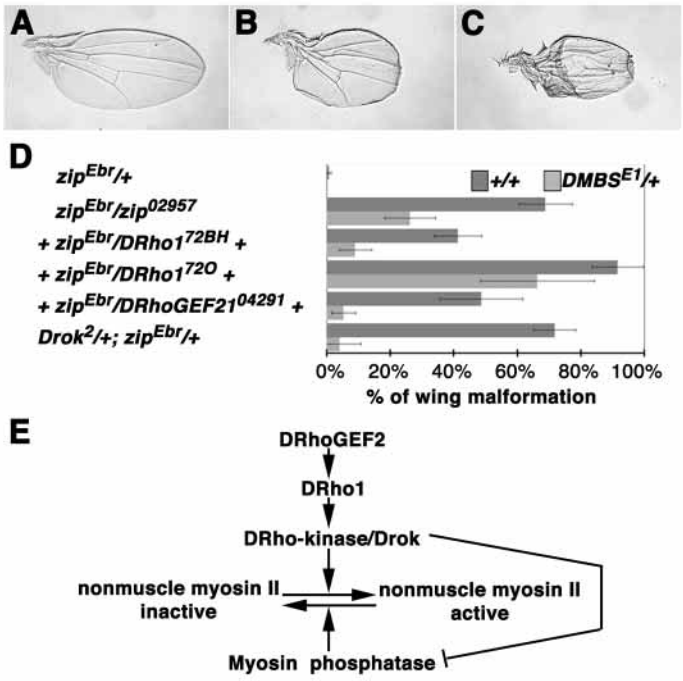

Fig. 8. *DMBS* genetically interacts with *zip* and with mutations in the components of the Rho signaling pathway. A partial defect of *zip* causes the malformed adult wing phenotype with a gradation in severity. (A) A wild type wing. (B,C) Wings of the *zip*^{Ebr}/*zip*^{02957} transheterozygotes. (D) Percentages of malformed wings in the flies with genotypes indicated on the left side of the panel. Heterozygosity for *DMBS*^{E1} significantly suppressed wing defects. (E) A model for the pathways regulating nonmuscle myosin II activation. See the text for the detail.

be heterozygous for *zip*^{Ebr}. As expected, the embryonic lethality was reduced to nearly half that of the corresponding cross (Fig. 7A). Similarly, the heterozygosity for *zip*^{Ebr} considerably suppressed lethality due to ectopic *DRhk*$^{+}$-expression (Fig. 7B). These results strongly suggest that either loss of *DMBS*$^{+}$ or overexpression of *DRhk*$^{+}$ causes hyperactivation of nonmuscle myosin II through increasing the levels of phosphorylation of MRLC.

zip^{Ebr} is a point mutation reported to be highly sensitive to genetic backgrounds (Halsell and Kiehart, 1998; Halsell et al., 2000). About 70% of the flies transheterozygous between *zip*^{Ebr} and *zip*^{02957} have malformed wings with varying degrees of severity (Fig. 8B-D). Although *zip*^{Ebr} is recessive, a considerable percentage of the flies heterozygous for both *zip*^{Ebr} and the mutations in the components of the Rho signaling pathway such as *DRho1* and *DRhoGEF2* produced similar defects (Fig. 8D) (Halsell et al., 2000). A half reduction of *Drok*, which encodes DRho-kinase (Winter et al., 2001), also dominantly enhanced *zip*^{Ebr}. This indicates the involvement of the Rho signaling pathway and its effector, DRho-kinase, in the myosin function of adult wing morphogenesis (Halsell et al., 2000). When the flies are also heterozygous for *DMBS*^{E1}, wing malformation is significantly suppressed (Fig. 8D), suggesting that DMBS functions antagonistically to the Rho signaling pathway (Fig. 8E) and is also involved in adult morphogenesis.

DISCUSSION

Involvement of DMBS in morphogenetic processes

The force-generating activity of nonmuscle myosin II is regulated mainly by phosphorylation and dephosphorylation of its regulatory light chain, MRLC. Myosin phosphatase is responsible for the negative regulation of nonmuscle myosin II through dephosphorylation of MRLC, and its regulatory myosin-binding subunit, MBS, is crucial in regulating the activity of myosin phosphatase and determining its substrate-specificity. Here we identified the mutants for the *Drosophila* gene encoding a homolog of MBS, DMBS. Genetic analyses of *DMBS* revealed its roles in dorsal closure during embryonic development and in adult wing morphogenesis. Extensive cell shape changes take place during both morphogenetic processes, and the genetic interactions with *zip* indicate the importance of DMBS in the regulation of nonmuscle myosin II in these processes. *DMBS* is expressed ubiquitously throughout development, and the mutants are lethal at early larval stages, suggesting yet other functions for DMBS during development.

Interactions with the Rho signaling pathway

The phenotype produced by overexpression of *DRhk*$^{+}$ resembles that of *DMBS* mutant embryos, and both phenotypes can be suppressed by reducing the gene dosage of *zip*$^{+}$. The results suggest that these phenotypes are the result of the hyperactivation of nonmuscle myosin II, and that myosin phosphatase and DRho-kinase function antagonistically toward each other in regulating nonmuscle myosin II (Fig. 8E). A similar observation has been reported for *let-502* and *mel-11* of *C. elegans*, which encode the homolog of Rho-kinase and MBS, respectively. The genes have been demonstrated to function in the hypodermal cell-shape change associated with the elongation of the embryo in *C. elegans* (Wissmann et al., 1997), thus indicating the conservation of the regulatory mechanisms of nonmuscle myosin II in morphogenesis. The genetic link between *zip* and the mutations in the Rho signaling pathway has been demonstrated (Halsell et al., 2000) (Fig. 8A-D), and this indicates the regulation of nonmuscle myosin II by the Rho signaling pathway. The suppression of both phenotypes generated by double heterozygosity for *zip* and the

mutations in the components of the Rho-signaling pathway by *DMBS* demonstrates that DMBS functions antagonistically toward the Rho-signaling pathway in the regulation of nonmuscle myosin II (Fig. 8E).

Roles of DMBS in dorsal closure

During dorsal closure, an extensive cell shape change in the lateral epidermis takes place. One of the major forces underlying the morphogenetic process is provided by the constriction of a supracellular purse-string revealed by the high level accumulation of F-actin and the heavy chain of nonmuscle myosin II along the leading edge of the lateral epidermis (Young et al., 1993) (Fig. 6D,G). We found that MRLC is also highly accumulated along the leading edge (Fig. 5D,E; Fig. 6G). Small quantities of these components of actomyosin are also detected along the inner surface of the plasma membrane. Phosphorylated MRLC was detected in significant amounts along the leading edge of the lateral epidermis (Fig. 5F and Fig. 6I), indicating that nonmuscle myosin II is persistently activated along the leading edge during extensive epidermal spreading.

In *DMBS* mutant embryos, the defects in dorsal closure seem to be confined to the leading edge cells, and these cells fail to fully elongate. In contrast, the lateral epidermal cells located more ventrally elongate more or less normally. It has been reported that dorsal closure is driven by multiple forces and that it can proceed in the absence of an intact contractile purse-string at the leading edge (Young et al., 1993; Kiehart et al., 2000). These lateral epidermal cells are under tension during dorsal closure (Kiehart et al., 2000), and they themselves may produce the forces to elongate.

It should be noted that the accumulation of nonmuscle myosin II in the leading edge cells was essentially not affected. Activation of nonmuscle myosin II takes place along the leading edge as in normal embryos, since the phosphorylated MRLC was detected there in the mutant embryos (Fig. 6H). In addition to the distribution along the leading edge, a significant accumulation of phosphorylated MRLC was detected also on the dorsal side of the boundaries between the leading edge cells in the mutant embryos (Fig. 6J). This may indicate the role of myosin phosphatase in inactivating nonmuscle myosin II in this subcellular location to coordinate elongation of the leading edge cells.

The results suggest the localized activation of myosin phosphatase during the normal course of dorsal closure. One possible explanation for this localized activation is that there is a subcellular distribution of myosin phosphatase itself in this region. However, a suitable antibody would have to be raised against DMBS to determine if this was so. Another possible explanation is the localization of an activator of myosin phosphatase in this region. Thus, there must be a subcellular localization of mechanisms for the regulation of nonmuscle myosin II. It has been demonstrated that the cellular polarity of the leading edge cells is altered from basolateral to apical in the leading edge during elongation (Ring and Martinez-Arias, 1993; Woods and Bryant, 1993; Fehon et al., 1994). It would be of interest to learn how cellular polarity affects the pattern of regulation of the nonmuscle myosin II in the leading edge cells. The results obtained in this study demonstrate the importance of both positive and negative regulation of nonmuscle myosin II in morphogenesis.

We are grateful to Drs. F. Matsumura, M. Mlodzik, J. Fristrom, R. Karess and L. Luo for the antibodies and the fly stocks. We also wish to thank T. Tsuboi and N. Minami for their technical assistance. This work was supported by grants from the Ministry of Education and Science of Japan, and the Japan Science and Technology Corporation.

REFERENCES

Alessi, D., MacDougall, L. K., Sola, M. M., Ikebe, M. and Cohen, P. (1992). The control of protein phosphatase-1 by targeting subunits. The major myosin phosphatase in avian smooth muscle is a novel form of protein phosphatase-1. *Eur. J. Biochem.* **210**, 1023-1035.

Amano, M., Ito, M., Kimura, K., Fukata, Y., Chihara, K., Nakano, T., Matsuura, Y. and Kaibuchi, K. (1996). Phosphorylation and activation of myosin by Rho-associated kinase (Rho-kinase). *J. Biol. Chem.* **271**, 20246-20249.

Arquier, N., Perrin, L., Manfruell, P. and Sémériva, M. (2001). The Drosophila tumor suppressor gene lethal(2)giant larvae is required for the emission of the Decapentaplegic signal. *Development* **128**, 2209-2220.

Brand, A. H. and Perrimon, N. (1993). Targeted gene expression as a means of altering cell fates and generating dominant phenotypes. *Development* **118**, 401-415.

Brown, N. H. and Kafatos, F. C. (1988). Functional cDNA libraries from Drosophila embryos. *J. Mol. Biol.* **203**, 425-437.

Fehon, R. G., Dawson, I. A. and Artavanis-Tsakonas, S. (1994). A Drosophila homologue of membrane-skeleton protein 4.1 is associated with septate junctions and is encoded by the coracle gene. *Development* **120**, 545-557.

Frangioni, J. V. and Neel, B. G. (1993). Solubilization and purification of enzymatically active glutathione S-transferase (pGEX) fusion proteins. *Anal. Biochem.* **210**, 179-187.

Fujioka, M., Takahashi, N., Odai, H., Araki, S., Ichikawa, K., Feng, J., Nakamura, M., Kaibuchi, K., Hartshorne, D. J., Nakano, T. and Ito, M. (1998). A new isoform of human myosin phosphatase targeting/regulatory subunit (MYPT2): cDNA cloning, tissue expression, and chromosomal mapping. *Genomics* **49**, 59-68.

Gotwals, P. J. and Fristrom, J. W. (1991). Three neighboring genes interact with the Broad-Complex and the Stubble-stubbloid locus to affect imaginal disc morphogenesis in Drosophila. *Genetics* **127**, 747-759.

Halsell, S. R., Chu, B. I. and Kiehart, D. P. (2000). Genetic analysis demonstrates a direct link between rho signaling and nonmuscle myosin function during Drosophila morphogenesis. *Genetics* **155**, 1253-1265.

Halsell, S. R. and Kiehart, D. P. (1998). Second-site noncomplementation identifies genomic regions required for Drosophila nonmuscle myosin function during morphogenesis. *Genetics* **148**, 1845-1863.

Hartshorne, D. J., Ito, M. and Erdodi, F. (1998). Myosin light chain phosphatase: subunit composition, interactions and regulation. *J. Muscle Res. Cell Motil.* **19**, 325-341.

Jordan, P. and Karess, R. (1997). Myosin light chain-activating phosphorylation sites are required for oogenesis in Drosophila. *J. Cell Biol.* **139**, 1805-1819.

Kaibuchi, K., Kuroda, S. and Amano, M. (1999). Regulation of the cytoskeleton and cell adhesion by the Rho family GTPases in mammalian cells. *Ann. Rev. Biochem.* **68**, 459-486.

Karess, R. E., Chang, X. J., Edwards, K. A., Kulkarni, S., Aguilera, I. and Kiehart, D. P. (1991). The regulatory light chain of nonmuscle myosin is encoded by spaghetti-squash, a gene required for cytokinesis in Drosophila. *Cell* **65**, 1177-1189.

Kawano, Y., Fukata, Y., Oshiro, N., Amano, M., Nakamura, T., Ito, M., Matsumura, F., Inagaki, M. and Kaibuchi, K. (1999). Phosphorylation of myosin-binding subunit (MBS) of myosin phosphatase by Rho-kinase in vivo. *J. Cell Biol.* **147**, 1023-1038.

Kiehart, D. P., Galbraith, C. G., Edwards, K. A., Rickoll, W. L. and Montague, R. A. (2000). Multiple forces contribute to cell sheet morphogenesis for dorsal closure in Drosophila. *J. Cell Biol.* **149**, 471-490.

Kimura, K., Ito, M., Amano, M., Chihara, K., Fukata, Y., Nakafuku, M., Yamamori, B., Feng, J., Nakano, T., Okawa, K. et al. (1996). Regulation of myosin phosphatase by Rho and Rho-associated kinase (Rho-kinase). *Science* **273**, 245-248.

Martinez-Arias, A. (1993). Development and patterning of the larval epidermis of *Drosophila*. In *The development of* Drosophila melanogaster.

pp. 517-608. Cold Spring Harbor Laboratory Press, Cold Spring Harbor, NY.

Matsumura, F., Ono, S., Yamakita, Y., Totsukawa, G. and Yamashiro, S. (1998). Specific localization of serine 19 phosphorylated myosin II during cell locomotion and mitosis of cultured cells. *J. Cell Biol.* **140**, 119-129.

Mizuno, T., Amano, M., Kaibuchi, K. and Nishida, Y. (1999). Identification and characterization of Drosophila homolog of Rho-kinase. *Gene* **238**, 437-444.

Neufeld, T. P. and Rubin, G. M. (1994). The Drosophila peanut gene is required for cytokinesis and encodes a protein similar to yeast putative bud neck filament proteins. *Cell* **77**, 371-379.

Noselli, S. (1998). JNK signaling and morphogenesis in Drosophila. *Trends Genet.* **14**, 33-38.

Ring, J. M. and Martinez-Arias, A. (1993). puckered, a gene involved in position-specific cell differentiation in the dorsal epidermis of the Drosophila larva. *Development*, **Suppl**. 251-259.

Sisson, J. C., Field, C., Ventura, R., Royou, A. and Sullivan, W. (2000). Lava lamp, a novel peripheral Golgi protein, is required for Drosophila melanogaster cellularization. *J. Cell Biol.* **151**, 905-917.

Staehling-Hampton, K., Hoffmann, F. M., Baylies, M. K., Rushton, E. and Bate, M. (1994). dpp induces mesodermal gene expression in Drosophila. *Nature* **372**, 783-786.

Strutt, D. I., Weber, U. and Mlodzik, M. (1997). The role of RhoA in tissue polarity and Frizzled signalling. *Nature* **387**, 292-295.

Tan, J. L., Ravid, S. and Spudich, J. A. (1992). Control of nonmuscle myosins by phosphorylation. *Ann. Rev. Biochem.* **61**, 721-759.

Winter, C. G., Wang, B., Ballew, A., Royou, A., Karess, R., Axelrod, J. D. and Luo, L. (2001). Drosophila rho-associated kinase (drok) links frizzled-mediated planar cell polarity signaling to the actin cytoskeleton. *Cell* **105**, 81-91.

Wissmann, A., Ingles, J., McGhee, J. D. and Mains, P. E. (1997). Caenorhabditis elegans LET-502 is related to Rho-binding kinases and human myotonic dystrophy kinase and interacts genetically with a homolog of the regulatory subunit of smooth muscle myosin phosphatase to affect cell shape. *Genes Dev.* **11**, 409-422.

Wissmann, A., Ingles, J. and Mains, P. E. (1999). The Caenorhabditis elegans mel-11 myosin phosphatase regulatory subunit affects tissue contraction in the somatic gonad and the embryonic epidermis and genetically interacts with the Rac signaling pathway. *Dev. Biol.* **209**, 111-127.

Woods, D. F. and Bryant, P. J. (1993). Apical junctions and cell signalling in epithelia. *J. Cell Sci.* **Suppl. 17**, 171-181.

Young, P. E., Richman, A. M., Ketchum, A. S. and Kiehart, D. P. (1993). Morphogenesis in Drosophila requires nonmuscle myosin heavy chain function. *Genes Dev.* **7**, 29-41.